A NETWORK THERMODYNAMIC APPROACH TO COMPARTMENTAL ANALYSIS

Na^+ TRANSIENTS IN FROG SKIN

D. C. MIKULECKY, E. G. HUF, AND S. R. THOMAS, *Department of Physiology, Medical College of Virginia, Richmond, Virginia 23298 U.S.A.*

ABSTRACT We introduce a general network thermodynamic method for compartmental analysis which uses a compartmental model of sodium flows through frog skin as an illustrative example (Huf and Howell, 1974*a*). We use network thermodynamics (Mikulecky et al., 1977*b*) to formulate the problem, and a circuit simulation program (ASTEC 2, SPICE2, or PCAP) for computation. In this way, the compartment concentrations and net fluxes between compartments are readily obtained for a set of experimental conditions involving a square-wave pulse of labeled sodium at the outer surface of the skin. Qualitative features of the influx at the outer surface correlate very well with those observed for the short circuit current under another similar set of conditions by Morel and LeBlanc (1975). In related work, the compartmental model is used as a basis for simulation of the short circuit current and sodium flows simultaneously using a two-port network (Mikulecky et al., 1977*a*, and Mikulecky et al., A network thermodynamic model for short circuit current transients in frog skin. Manuscript in preparation; Gary-Bobo et al., 1978). The network approach lends itself to computation of classic compartmental problems in a simple manner using circuit simulation programs (Chua and Lin, 1975), and it further extends the compartmental models to more complicated situations involving coupled flows and nonlinearities such as concentration dependencies, chemical reaction kinetics, etc.

INTRODUCTION

Living systems are highly compartmentalized, and compartmental analysis is an integral part of their study. The literature dealing with this subject as an approach to biological systems is growing steadily. This paper has three objectives:

(*a*) Our major objective is to demonstrate that compartmental analysis fits naturally into the recently evolved marriage of nonequilibrium thermodynamics and kinetics known as "network thermodynamics." The organization of a system, its topology, has always been central in any successful compartmental analysis.[1] Network thermodynamics has grown out of the recognition that along with the molecular properties of membranes and other structures, organization contributes in an essential way to the global behavior of organized, highly structured systems such as those commonly found in living tissue. Thus, because network thermodynamics has developed explicit techniques for analyzing organized systems and in addition can deal with a much broader class of problems, it is fitting that it be recog-

[1]Huf, E. G., and J. R. Howell. Topological aspects of Na^+ saturation kinetics in frog skin. Submitted for publication.

nized as a paradigmatic approach to compartmental analysis. Among the advantages of the network approach is the availability of a wide variety of circuit simulation programs (Chua and Lin, 1975; Blattner, 1976; Kaplan, 1975) and the ability to extend an analysis beyond simple compartmental analysis to the study of coupled flows by introducing multiport elements. (A port is a pair of input-output pathways through a structure, such as a membrane. An ordinary electrical resistor is a one-port whereas a transformer is a two-port.) The analysis can be extended to include chemical reactions (Wyatt, 1978).[3] Besides these advantages, the network approach has its basis in dynamic systems theory and thereby opens doors to some of the most modern mathematical tools available (Oster and Perelson, 1974*a* and *b*; Heinrich et al., 1977; Welch, 1977). It is also true that some of these approaches are being rediscovered independently in compartmental analysis (e.g., Cobelli et al., 1977; Sandberg, 1977), but these works fail to recognize the applicability of a large body of theory that already exists in the literature of electrical engineering and the related areas of dynamic systems theory. The ability of the network approach to unify should provide a certain economy in the theoretical foundations of a number of closely related areas of endeavor, including compartmental analysis.

(*b*) Our second objective is to provide a simple method for setting up and solving problems in compartmental analysis, using network diagrams and circuit simulation programs.

(*c*) Our third objective is to demonstrate the method's effectiveness using as an example of a multicompartment system a compartmental model of sodium flow in frog skin (Huf and Howell, 1974*a* and *b*, 1976, 1977; Howell and Huf, 1974, 1976, 1977). Although this multicompartment model is not universally accepted as a completely accurate picture of sodium movement in frog skin, it is sufficiently detailed and versatile to be interesting as an example of our analytic technique. What is more, the technique allows for severe modification with minimum effort so that other models can easily be made to test alternative pictures of how frog skin is organized. We hope that other workers will adapt the model to their needs.

As a first step and a test of the method, the network discussed in detail below for simulating the compartmental analysis of the frog skin was used to reproduce some of the published results of Huf and Howell. Having duplicated a sufficient number of these already well-established aspects of the Huf and Howell compartmental model, we apply the network approach to a series of experiments involving low concentration pulses of labeled sodium on the outside of the skin as an extension of Huf and Howell's backflux simulations. In related papers, the work on this compartmental model of sodium flows in frog skin is related to measured short circuit current (that is, the current between baths clamped at zero potential difference). This is accomplished by developing an electrochemical two-port element, i.e., an element with two sets of flow-force variables which can, in general, interact. In the case of frog skin and other epithelia, voltage-current and salt flow-concentration difference are coupled by the transference number which explicitly expresses the contribution to the total current from the salt's concentration distribution (Mikulecky, 1978).[2] By the introduction of the electrochemical two-port, the relation of sodium movement and concentration to electrical effects is modeled, and certain disadvantages of the equivalent circuit approach

[2] Mikulecky, D. C. 1979. A network thermodynamic two-port element to represent the coupled flow of salt and current. An improved alternative for the equivalent circuit. *Biophys. J.* In press.

(Finkelstein and Mauro, 1963) are overcome. The electrochemical two-port is analogous to the two-port element introduced for coupled solute and volume flow (Mikulecky, 1977). The two-port for coupled solute and volume flow has a natural piecewise linearization (Thomas and Mikulecky, 1978*a*) and has been applied to epithelial transport (Thomas, 1977; Thomas and Mikulecky, 1978*b* and *c*).[3] These properties are also relevant to the electrochemical two-port. This series of works illustrates how the network approach to compartmental analysis can be readily extended to include further information about the system, such as the effect of additional, coupled flows, and their driving forces. This compartmental model, its topology, and the values of its resistances and capacitances serve as a basis for the more extensive model (Mikulecky et al., 1977*b*; Mikulecky and Thomas, 1977).[4] In future work, the electrochemical two-port will be replaced by a multiport element to incorporate explicitly the contribution of other ions such as potassium. This aspect of the network thermodynamic paradigm is one of its strongest. The ease with which the networks can be elaborated (or reduced) in detail and complexity while preserving their 1:1 relation to tissue morphology is an extremely potent feature. Network models are thus readily adapted to future experimental findings or alternative concepts about the system being studied and can be a great aid in designing experiments as well.

The compartmental model and/or the multiport networks derived from it, once translated into networks, lend themselves to direct analysis by use of a circuit simulator (Blattner, 1976; and Kaplan, 1975). We have used ASTEC2 (Barocas, 1977), a simulation program created in France. It has a capacity for nonlinear multiport circuit elements to be introduced by using FORTRAN to define the constitutive relations ("current-voltage characteristics"). This provides a great deal of flexibility, as the simulation is done from the specified network topology (schematic diagram) and a specification of the nonlinear constitutive relations, plus appropriate parameters for the resistances, capacities, and sources. Once the FORTRAN description is completed, no further equations need be written, because the simulation program sets them up automatically. Recently, some of the simulations were successfully repeated using SPICE2 (Chua and Lin, 1975; Blattner, 1976; Kaplan, 1975). Simulation programs for compartmental analysis also exist which do roughly the same thing, but thus far only for single, uncoupled flows. Preliminary versions of this work on compartmental analysis have already appeared (Mikulecky and Thomas, 1977; Huf et al., 1978).

FROM THE CLASSICAL COMPARTMENTAL ANALYSIS TO NETWORK THERMODYNAMICS

For an example, we will examine the simple diffusion of a substance between two compartments separated by a membrane, as shown in Fig. 1 *A*. The two compartments are labeled L and R, and the amounts of the diffusible material in each will be symbolized by S_L and S_R, respectively. The rates of change of the amounts of the diffusing material in each com-

[3]Mikulecky, D. C., and S. R. Thomas. Some network thermodynamic models of coupled dynamic physiological systems. *J. Franklin Inst.* In press.

[4]Mikulecky, D. C., S. R. Thomas, C. M. Gary-Bobo, H. Godeau, and J. Wietzerbin. A network thermodynamic model for short circuit current transients in frog skin. Manuscript in preparation.

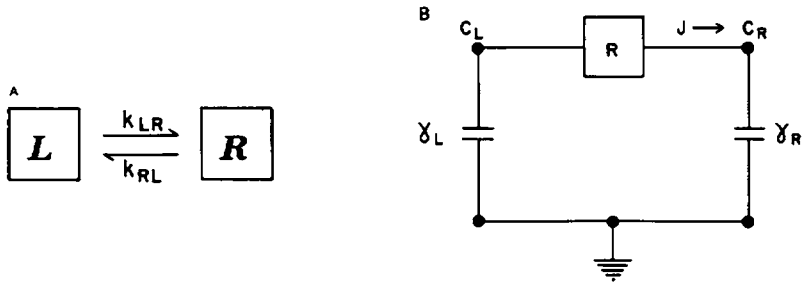

FIGURE 1 Two representations of simple diffusion across a membrane separating two finite baths. (Membrane is in a steady state, but the baths are not). (A) The compartmental analysis representation. The boxes R and L represent the two compartments, and the rate constants and arrows, the forward and the backward fluxes. (B) The network representation. The resistor represents the membrane, the node voltages, C_L and C_R, represent the time-dependent concentrations of the baths, γ_L and γ_R are capacitors representing the ratio of membrane area to bath volume.

partment $\dot{S}_L$ and $\dot{S}_R$ are described by the equations,

$$\dot{S}_L = -k_{LR}S_L + k_{RL}S_R = -\dot{S}_R, \tag{1}$$

where the rate constants k_{LR} and k_{RL} govern the unidirectional exchange of material. In the network formulation, the amount of material, S_i, in compartment i is analogous to the amount of charge on a capacitor. Concentration is analogous to potential, and permeability is analogous to conductance, so that the force-flow relationship of Fick's law is isomorphic with the conductance form of Ohm's law. By generalizing the concept of capacitance beyond the purely electrical effect of charge storage on a surface to the storage and/or depletion of material in various compartments ("pools" as they are often called), time-dependent processes are easily modeled in a network. (Mikulecky et al., 1977*b*; Wyatt, 1978). Wyatt has also given a clear discussion of the difference between the dissipation associated with resistive elements in a network and the reversible energy storage associated with capacitive elements. Thus, as Wyatt points out, the study of steady states is the study of resistors, whereas the study of equilibrium is the study of capacitors. The volume of a compartment (V_i) acts as a generalized static capacitance in relating the amount of material (S_i) in the compartment to the concentration (C_i) of the material in that compartment,

$$V_i = \frac{S_i}{C}. \tag{2}$$

It is a simple transformation to rewrite Eq. 1 as Fick's law and thus achieve an analogy with Ohm's law for a network. The rate coefficients (which have units of min^{-1}) are related to membrane permeability (P in liters $\cdot$ cm^{-2} $\cdot$ min^{-1}), area of the membrane (A in cm^{-2}), and compartment volumes in liters, by the expressions

$$k_{LR} = PA/V_L, \tag{3a}$$

and

$$k_{RL} = PA/V_R. \tag{3b}$$

Using Eqs. 2 and 3, Eq. 1 can be rewritten

$$\dot{C}_L - \dot{C}_R = \dot{\Delta C} = -P\Delta C(A/V_L + A/V_R), \tag{4}$$

or, if the net flux through the membrane (in moles · cm^{-2} · min^{-1}) is $J = P\Delta C$, Eq. 4 can be written in the form,

$$\dot{\Delta C} = (A/V_L + A/V_R)J. \tag{5}$$

For the purpose of simulation, it is convenient to define the dynamic capacitances γ_L and γ_R to be compatible with the fluxes rather than flows, in contrast to the static capacitance in Eq. 2 above,

$$\gamma_L = V_L/A \tag{6}$$

and

$$\gamma_R = V_R/A \tag{6}$$

so that

$$\dot{\Delta C} = -(1/\gamma_L + 1/\gamma_R)J. \tag{7}$$

As a simple network, the example above is shown in Fig. 1 B. Note that, diagrammatically, the nodes represent compartment values of concentrations (potential analogs), and the branches represent elements (membranes) between the compartments (resistor analogs) or the capacitances which depict the storage capacity of each compartment. The net flow of material between the compartments is the analog of current. Using the constitutive relations for capacitors γ_L and γ_R and Kirchoff's current law, which, in this case, states that the transmembrane flow is equal to the flow through each capacitor, Eq. 7 above is readily obtained directly from the network and describes the nonsteady-state filling and/or depletion of the compartments. Also, the analogy between Fick's and Ohm's laws is seen in the relationship between Eqs. 7 and 4. Thus, by using the network diagram in Fig. 1 B, an analysis of the compartmental problem defined by Fig. 1 A can be obtained very simply.

Eq. 1 is more general than Fick's law if $k_{LR}V_L \neq k_{RL}V_R$. This asymmetry in rates reflects some source of energy driving the process, such as active transport or solvent drag (e.g., see Mikulecky, 1977). Passive transport not coupled to another process is described by equal forward and backward rates. When $k_{LR}V_L = k_{RL}V_R$, the membrane is a reciprocal element and can be modeled by a simple one-port resistor (Mikulecky et al., 1977*b*). Helman and Fisher (1977) modeled an asymmetry in forward and backward rates (rectification) by using diodes in an equivalent circuit representation. This configuration should not be interpreted as passive, as the representation is equivalent to the elements defined below for active transport systems, and can "pump" up gradients. Energetically, the creation of such asymmetrical forward and backward rates implies a source of energy and cannot be both passive and uncoupled from other flows.

For the case of asymmetric rate constants ($k_{LR}V_L \neq k_{RL}V_R$), we introduce an element that is functionally the set of unidirectional one-ports shown in Fig. 2. The nature of the unidirectional sources is a matter of convenience for simulation. Because ASTEC2 would not compute with node voltages (on the other hand SPICE2 will), resistors R of sufficient

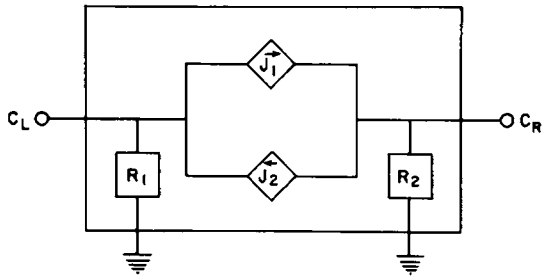

FIGURE 2 A two-port element for simulating flow between two compartments with asymmetric rate constants using ASTEC2 (explanation in text).

size were inserted to assure that the magnitude of the current to ground was always negligible. These resistors then served as "potentiometers" measuring the node potentials C_L and C_R for the FORTRAN functions defining J_1 and J_2.

THE COMPARTMENTAL MODEL OF FROG SKIN

To illustrate the virtues of the network approach, we chose an example of sufficient detail and versatility. It also has been subjected to extensive computation and serves as a good bench mark for our new method. The functional organization of frog skin has been viewed in other ways (e.g., see Farquhar and Palade [1965] or Rick et al. [1978]), and these alternative pictures of the frog skin can be modeled as a network equally well. Huf and Howell (1976) modeled the organization of the frog skin as shown diagrammatically in Fig. 3, and translated this into the system of compartments shown in Fig. 4. In this model, the bulk of the sodium is assumed to be evenly distributed over the "remaining epithelial cells," represented by compartment 4. A small fraction of the epidermal sodium is placed in a "transepidermal sodium transport compartment," represented by compartment 3. This may or may not be the so-called first reacting cell layer. The essential point here is that the model shows a "transepidermal transport compartment, 3" and a "Na-maintenance compartment, 4." The functional relationship between these two sodium compartments has been explored in the computer study by Howell and Huf (1975) where variations in the total epidermal sodium content were systematically varied (see Table 2 of the cited paper). One set of values used agrees with those in the recently published paper by Rick et al. (1978), who by the electronmicroprobe technique have found the very low value of 9 mM for

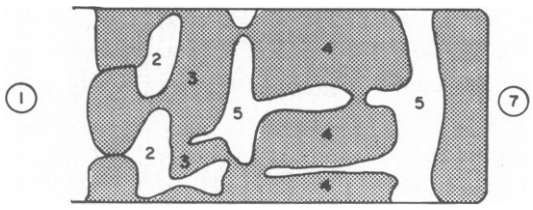

FIGURE 3 A schematic diagram of the organization of frog skin. 1. Outer bathing solution; 2. subcorneal space; 3. first reacting cell layer; 4. remaining cellular compartment; 5. extracellular space; 7. inner bathing solution.

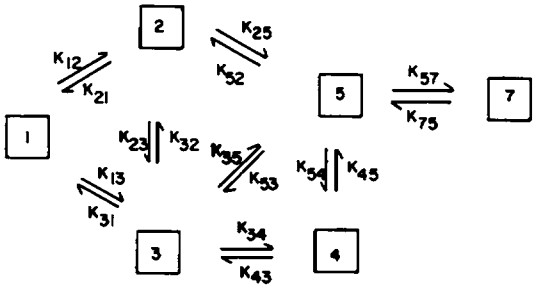

FIGURE 4 Compartmental analysis representation of frog skin. Compartments are: 1. Outer bathing solution; 2. subcorneal space; 3. first reacting cell layer; 4. remaining cellular compartments; 5. extracellular space; 7. inner bathing solution.

the mean cellular sodium concentration. The considerable discrepancies in the data in the literature on the epidermal sodium content are very disturbing at this time, and they remain to be resolved. Nevertheless, because the technique we are presenting is so versatile, it can easily be modified to reflect new or alternative pictures of the system's organization.

We readily translated the compartmental model into the network shown in Fig. 5. E_1 and E_2 can be either potential sources, when the baths are clamped at a constant concentration, or capacitors, when they are allowed to change concentration. The resistors are all passive elements, and $G1$ and $G2$ are the strong and weak pumps of Huf and Howell's model in the form of a pump-leak system. Their representation as a network element is shown in Fig. 6. These elements and the resistors in parallel convert the asymmetric forward and backward rate constants into a pump-leak system with unidirectional pumps $G1$ and $G2$, in parallel with the passive leak represented by the parallel resistors. The values of the various components are listed in Table I. All have been calculated to conform to the Huf and Howell model with two exceptions: (*a*) the baths in their model were finite, whereas these are infinite and are therefore represented by ideal potential sources, and (*b*) the size of the first reacting

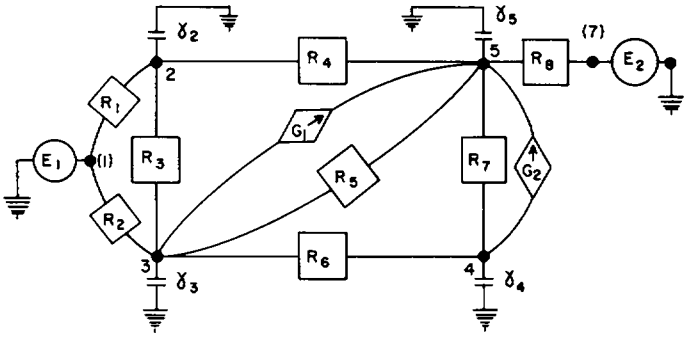

FIGURE 5 Network representation of frog skin. E_1, potential source clamping concentration of labeled sodium in outer bath. Nodes: 1. Outer bathing solution; 2. subcorneal space; 3. first reacting cell layer; 4. remaining cellular compartment; 5. extracellular space. E_2, potential source clamping concentration of labeled sodium in inner bath; γ_i, capacitors representing ratio of membrane area to volumes of the unclamped compartments; R_i, resistors representing rate constants for the passive filling and emptying of compartments; G_i, active transport pumps (dependent sodium flow sources as in Fig. 6). Values of the R_i, C_i, and G_i from Table I and Appendix I.

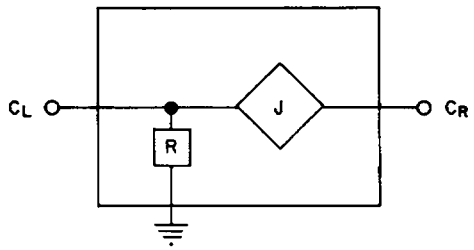

FIGURE 6 Network element for active sodium flow. R is a very large resistance which acts as a potentiometer to determine C_L relative to ground. J is a dependent flow source having the characteristics explained in Appendix I.

cell layer is twice that of their model in order to better fit the short circuit current data modeled by the electrochemical two-port (Mikulecky et al., 1977*a* and footnote 4).

Simulations were first performed with a network identical to that obtained from Huf and Howell's model in order to test the method. For their models 10E (no shunt, i.e., a paracellular pathway from subcorneal space to extracellular space) and 10Es (shunt present) under conditions for determining forward, backward, and net fluxes with pumps present and absent (ouabain effect), the network simulation matched the published data (Huf and Howell, 1974*a* and *b*, 1976) for four significant figures. The networks of the slightly altered model also give qualitatively the same behavior as the original Huf and Howell model with

TABLE I
PARAMETERS USED IN THE NETWORK MODEL VALUES

Parameter	Model 10E	Model 10Es
R1 in SCS	1.25×10^{6}*	1.25×10^{6}
R2 in FRCL	1.0×10^{7}	1.0×10^{7}
R3 SCS-FRCL	1.0×10^{7}	1.0×10^{7}
R4 shunt	Open	1.25×10^{8}
R5 FRCL-ECS	2×10^{7}	2×10^{7}
R6 FRCL-RCC	5×10^{7}	5×10^{7}
R7 RCC-ECS	1×10^{6}	1×10^{6}
R8 ECS-OUT	5×10^{5}	5×10^{5}
G1 strong pump (FRCL → ECS)	2×10^{5}‡	2×10^{5}
G2 weak pump (RCC → ECS)	1×10^{6}	1×10^{6}
γ^2 SCS	2×10^{-7}	2×10^{-7}
γ^3 FRCL	5×10^{-7}	5×10^{-7}
γ^4 RCC	4×10^{-6}	4×10^{-6}
γ^5 ECS	5×10^{-7}	5×10^{-7}
E2 inner bath	115§	115
E1 outer bath	Step (see text)	Step (see text)

*Resistance calculated from Huf and Howell (1976) using $R_k = 1/V_i k_{ij} = 1/V_j k_{ji}$. For example, $R_1 = 1/V_1 \cdot k_{12} = 1/(5 \times 10^{-3})(16 \times 10^{-5})$ where i stands for the node or compartment on one side of branch k, and j the node or compartment on the other side. These "resistors" correspond to the reciprocal of the conductances, P, in Eq. 4 and have conductance $(1/R)$ units of liters · centimeters^{-2} · minutes^{-1} as the fluxes (including the "pumps") are in moles · centimeters^{-2} · minutes^{-1}, and the node potentials (concentrations) are in moles · liters^{-1}.
‡The values of these pump resistors were determined by the procedure in Appendix I. The capacitances are in units of centimeters^2 · liters^{-1} and correspond to the definition given in Eq. 6.
§The units of the potentials (in reality bath concentrations) are in millimolars.

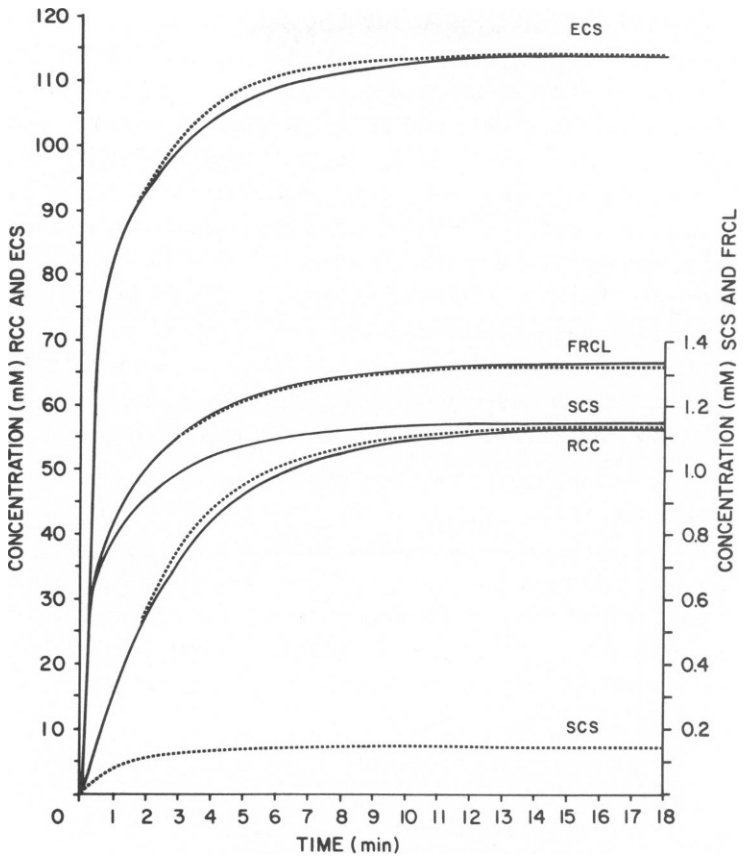

FIGURE 7 The approach to stationary state concentrations of labeled sodium with 115 mM cold sodium outside and 115 mM labeled sodium inside; for the compartments SCS (subcorneal space), FRCL (first reacting cell layer), RCC (remaining cellular compartment), and ECS (extracellular space). Values from model 10Es (with shunt pathway) are shown as solid lines, those for 10E (shunt pathway absent) are shown by broken lines.

slight quantitative differences. The experimental condition to be simulated here is a variation on Huf and Howell's backflux simulations (Morel and LeBlanc, 1975; Gary-Bobo et al., 1978; and footnote 4). The first 40 min are as in the backflux simulation with the exception that the bath concentrations are held constant, i.e., the outer bath is held at zero-labeled sodium and 115 mM cold sodium and the inner bath at 115 mM labeled sodium concentration.[5] At the end of the first 40 min, a square-wave pulse of labeled sodium is given in the outer bath with the total (cold + label) always 115 mM, while the inner bath is held at 115 mM labeled sodium as before. This pulse lasts 40-min. After that (80 min from the start), the initial conditions are restored, i.e., zero-labeled sodium and 115 mM cold sodium in the outer bath and the inner bath still held at 115 mM labeled sodium. In every simulation,

[5]Experimentally, this would be better expressed in terms of specific activity, but conceptually, the idea of a concentration of labeled sodium is consistent with the use of a capacitive constitutive relation as done through this work. Thus, all experimental conditions and results are in terms of labeled sodium concentration.

ASTEC2 was supplied with the network diagram in Fig. 5, the parameter values in Table I, and the bath concentrations (constant for the inner bath, a square pulse for the outer bath). ASTEC2 then computed all the compartment concentrations and all fluxes between compartments (of labeled sodium). (Because ASTEC is an expensive program and not generally available, Appendix II describes the simulation program used on SPICE2, which is similar.) Fig. 7 shows the result of the simulation of the concentrations of labeled sodium in the various compartments for model 10E (no shunt) and 10ES (shunt present) during the first 40 min, the period resembling Huf and Howell's backflux simulation. The presence of the shunt has a significant effect only on the concentration of labeled sodium in the subcorneal space. The other compartment concentrations show only slight alteration.

Unless otherwise indicated, for the remainder of this paper we will consider the model 10Es, which has the shunt pathway in it. The concentration changes of labeled sodium accompanying the labeled sodium pulse in the outer bath are shown for three different sized

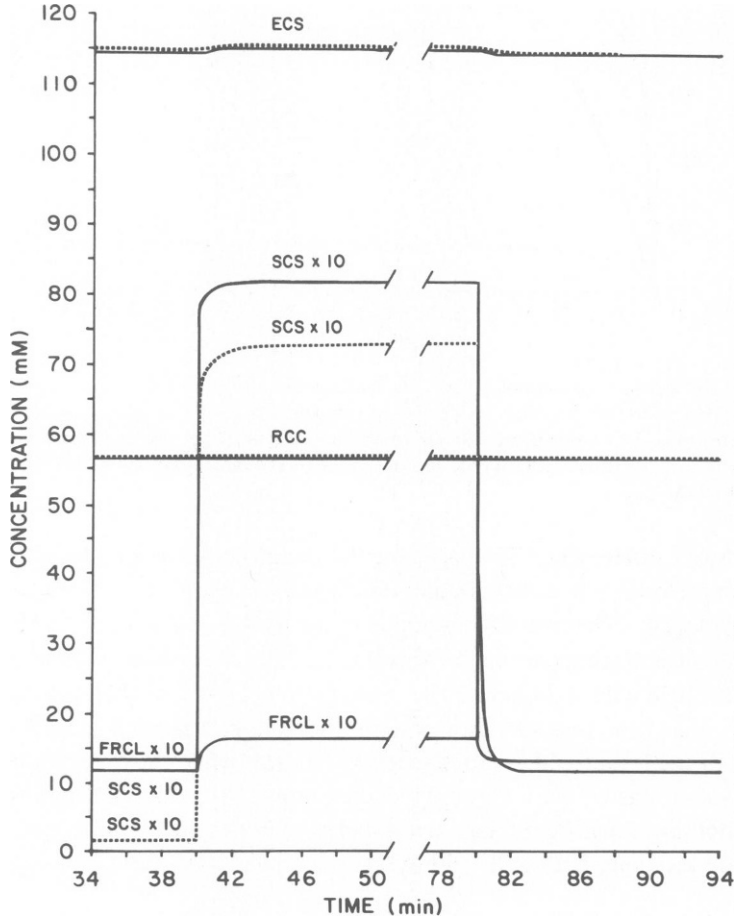

FIGURE 8 Concentrations of labeled sodium in the four compartments during a 40-min pulse of 115 mM labeled sodium in the outer bath preceded and followed by 40 min of zero-labeled sodium in a background of 115 mM cold sodium. The inside bath is at 115 mM labeled sodium throughout.

pulses in Figs. 8–10. In the case of 115 mM pulse (Fig. 8), all internal compartment concentrations of labeled sodium are altered by the pulse. In the paper using the two-port for salt and current (Gary-Bobo et al., 1978,; and footnote 4), the concentration dependence of the conductance, permeability, and transference number was taken into account along with the Michaelis-Menten properties of the conductance (saturability). This explicitly acknowledges the fact that the skin bathed by 115 mM sodium on the outside as simulated here can be expected to differ from a skin bathed outside by a solution low in total sodium. Fig. 9 shows that with a smaller pulse of labeled sodium in the outer bath (8 mM) the effect is mainly to alter the concentrations of labeled sodium in the subcorneal space and the first reacting cell layer. With a still smaller pulse (0.5 mM, Fig. 10), the effect is only significant in the subcorneal space. These results tend to add additional substance to the analysis of Morel and LeBlanc (1975), which concluded that the observed short circuit current during

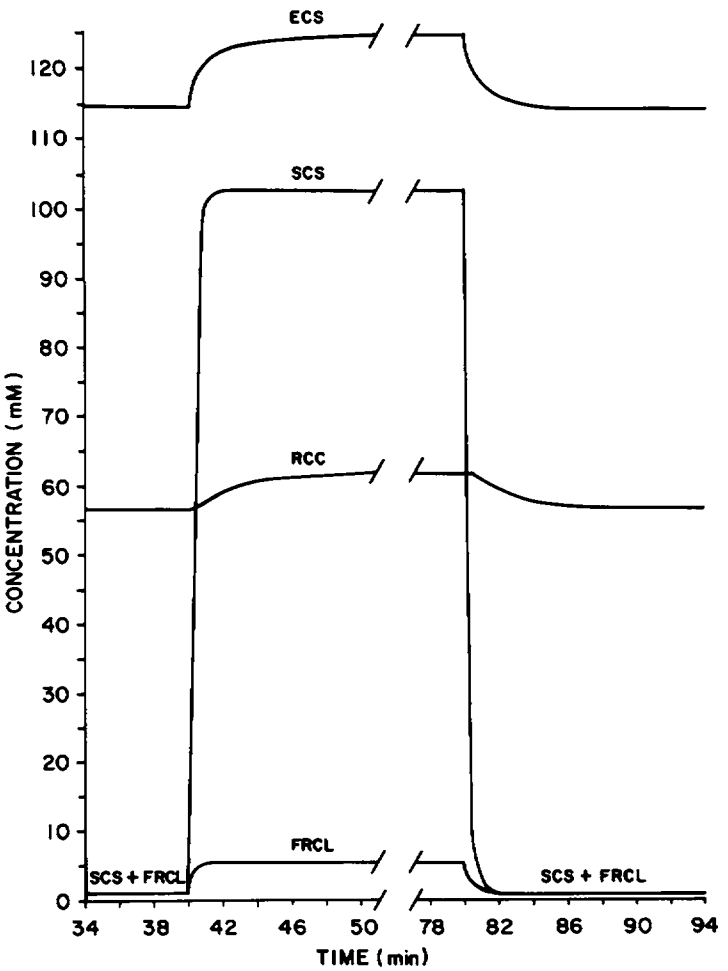

FIGURE 9 Concentrations of labeled sodium of the four compartments during a 40-min pulse of 8 mM labeled sodium in the outer bath. Solid lines are for model 10Es and broken lines for model 10E. 115 mM labeled sodium inside throughout.

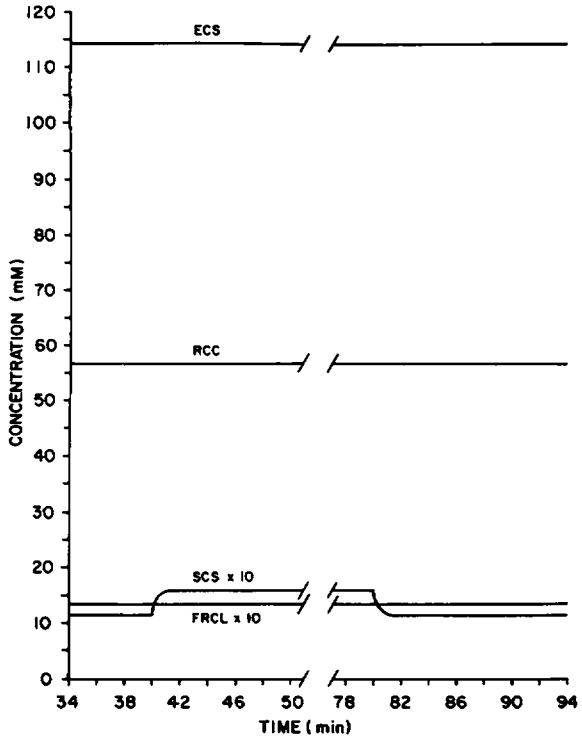

FIGURE 10 Concentrations of the four compartments during a 40-min pulse of 0.5 mM labeled sodium in the outer bath with 115 mM labeled sodium inside.

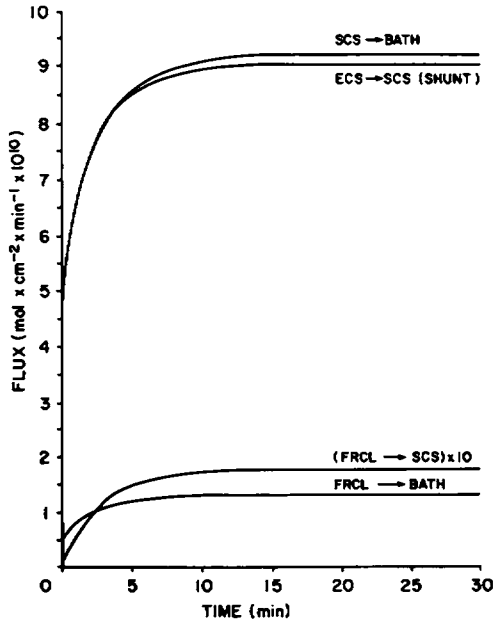

FIGURE 11 Time-course of fluxes during initial period with zero-labeled sodium in outer bath and 115 mM labeled sodium inside. Model 10Es.

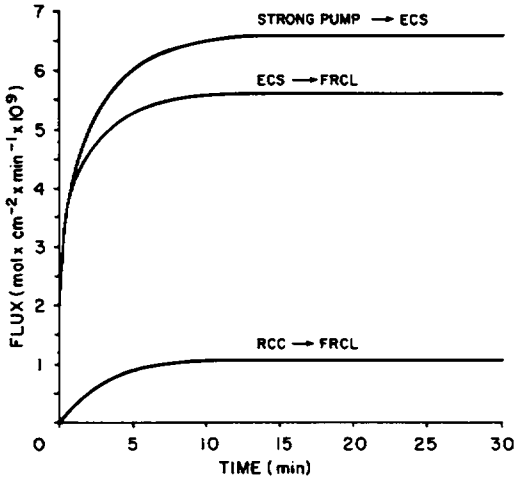

FIGURE 12 Time-course of fluxes during initial period with zero-labeled sodium in outer bath and 115 mM labeled sodium inside. Model 10Es.

low sodium pulses (ca. 7.2 mM) under somewhat different conditions reflected the properties of select barriers within the skin. The rationale behind the continuation of the low sodium transient measurements (Mikulecky et al., 1977*a*; Gary-Bobo et al., 1978, and footnote 4) is that, initially, the short circuit current measures events involving sodium movement across the apical membrane. The model suggests that this is true in part even in the case of a pulse of labeled sodium; however, as will be shown in the analysis of the flows during the pulse, the filling of the subcorneal space is the major component.

The initial "charging" fluxes during the first 40 min are shown in Figs. 11–13. The fluxes of labeled sodium all increase monotonically to their steady-state levels except for the flux from the inner bath to the extracellular space (ECS) and the flux from the ECS to the re-

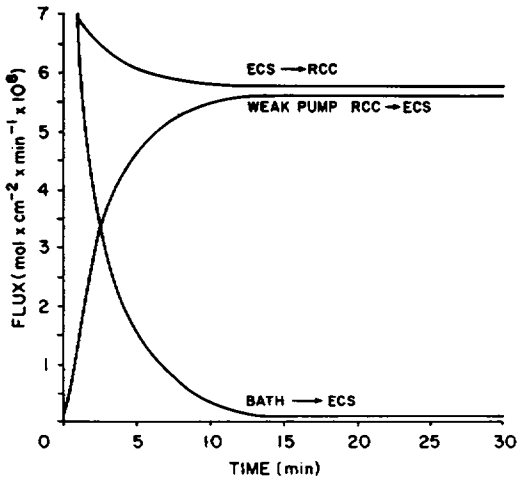

FIGURE 13 Time-course of fluxes during initial period with zero-labeled sodium in outer bath. Model 10Es.

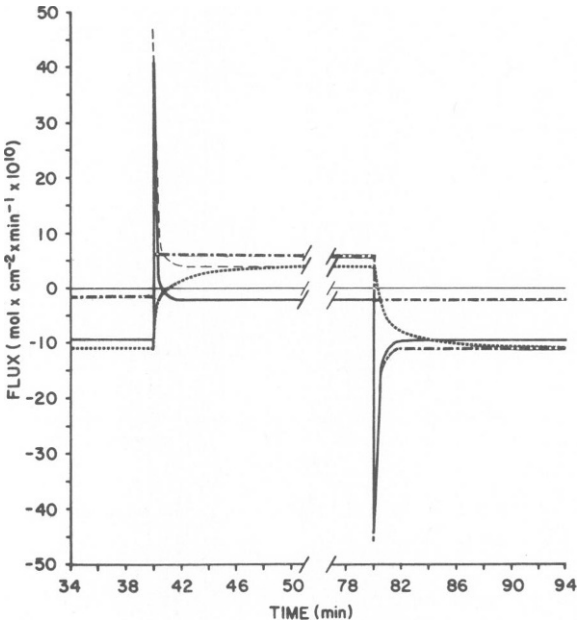

FIGURE 14 Influxes and effluxes during 40-min pulse of 8 mM labeled sodium and 107 mM cold sodium in outer bath. Inner bath with 115 mM labeled sodium. Model 10Es. Solid line is influx from outer bath to SCS. Heavy broken line is influx to FRCL. Broken line is total influx. Dotted line is efflux to inner bath.

maining cell compartment (RCC) (Fig. 13). These latter two fluxes have a large early maximum and then decay to their steady-state values (the initial increase in these fluxes is not shown in the figure.). On the other hand, during the 40-min labeled sodium square-wave pulse in the outer bath, there is an "on-off" type peak associated with the influxes from the outer bath, with entry into the subcorneal space dominating. Figs. 14 and 15 show the influx (solid line) and the efflux (dotted line) pulses of labeled sodium in the shunted and nonshunted cases. The total influx, dominated by the influx to the subcorneal space, results in a sharp spike of flux at the beginning and end of the pulse of labeled sodium in the outer bath. Fig. 16 shows that this behavior persists for a pulse as large as 115 mM. Thus, the technique of applying a pulse of labeled sodium on the outer surface of the frog's skin produces a transient in labeled sodium flux into the skin similar to that observed for short-circuit current under somewhat similar circumstances (Morel and LeBlanc, 1975). In related works, it is shown that these two events can be correlated even more strongly by the use of the electrochemical two-port coupling the sodium flux to the electric current flux. In that analysis, the saturability of the short circuit current has also been analyzed along with the concentration dependence of the conductance and transference number. At present there is sufficient reason to believe that the influx is responsible for the qualitative features of the short-circuit current transient during pulses of labeled sodium in the outer bath of any magnitude for any system similar to that modeled by this network.

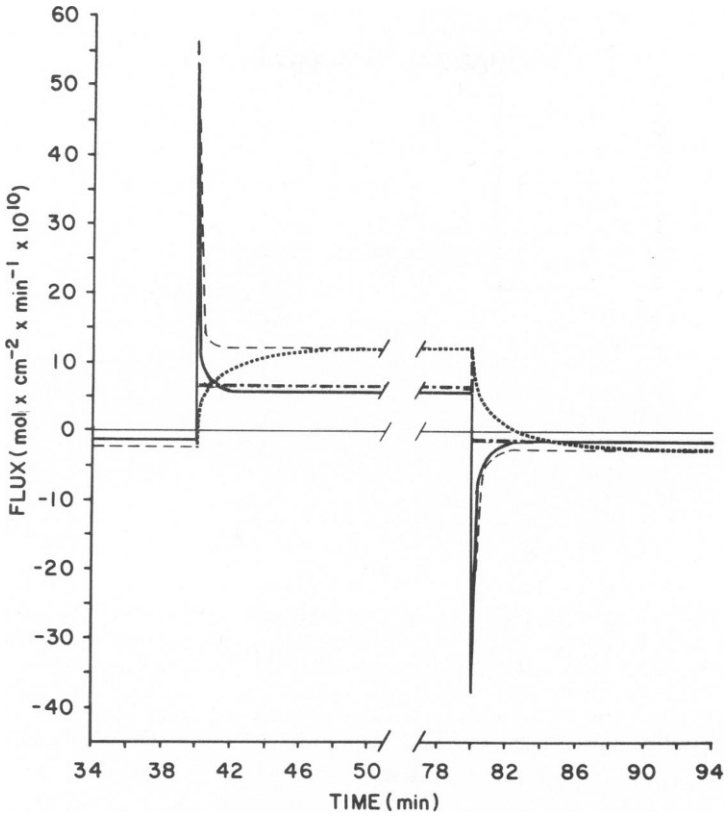

FIGURE 15 Influxes and efflux during 40-min pulse of 8 mM labeled and 107 mM cold sodium in outer bath. Inner bath contains 115 mM labeled sodium. Model 10E. Solid line is influx from outer bath to SCS. Heavy broken line is influx to FRCL. Broken line is total influx. Dotted line is efflux to inner bath.

SUMMARY AND CONCLUSIONS

Using a circuit simulation program, we carried out compartmental analysis of labeled sodium movement through frog skin under conditions that resemble those previously observed experimentally. The numerical values for the simulation network's elements were obtained from Huf and Howell's (1976) model. The results obtained required only that the network topology and the various values of the elements be specified. Results for simulations already carried out by Huf and Howell were matched to four significant figures, and further calculations were performed to model the labeled sodium pulse experiments. From these additional simulations, we were able to establish that the labeled sodium pulse experiments mainly probe the influx of labeled sodium at the outer surface of the skin. Further work introduces two-port elements to investigate the coupled fluxes of sodium and current. In that case, a more direct link between the sodium influx and transepithelial short circuit current is established.

Although this demonstration of the method focused on a particular model as an example,

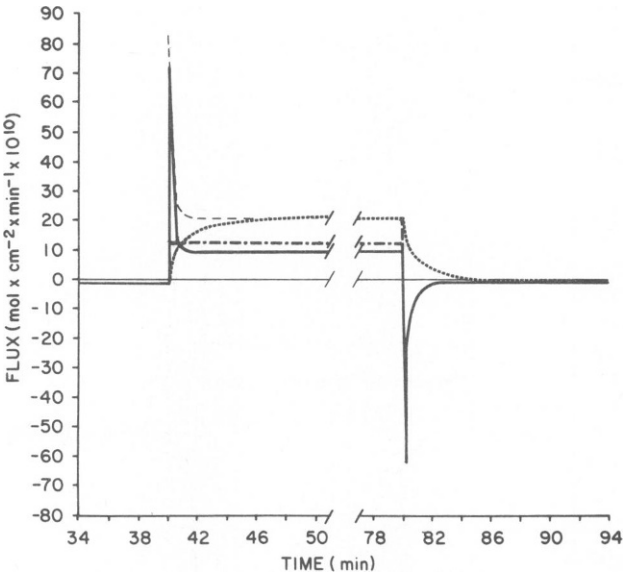

FIGURE 16 Influxes and efflux during 40-min pulse of 115 mM labeled sodium in outer bath. Inner bath contains 115 mM labeled sodium. Model 10Es. Solid line is influx from outer bath to SCS. Broken line is influx to FRCL. Heavy broken line is total influx. Dotted line is efflux to inner bath.

it is easy to apply the same techniques to any model. With a SPICE2 user's manual and Appendix II one could easily model a system of his choice.

First of all, thanks to C. M. Gary-Bobo, H. Goudeau, and J. Wietzerbin for their patience and tolerance in familiarizing us with the experimental details so necessary for our simulation work. The Department of Biology of the Commissariat l'Energie Atomique (CEA), Saclay, France, very generously supported the computer work and introduced us to ASTEC2. Also, thanks to the Medical College of Virginia and North Atlantic Treaty Organization (grant #1239) for making it possible for two of us (D.C.M. and S.R.T.) to go to France to do part of the work.

Received for publication 17 March 1978 and in revised form 9 September 1978.

APPENDIX I

Comparison of the Pump-Leak Model for the Pumps with the Unidirectional Fluxes of Compartmental Analysis

The network simulation used here models the flows between the two cellular compartments and the extracellular space as pump-leak systems. The compartmental analysis of Huf and Howell (1976), from which the parameter values were taken, used asymmetric forward and backward rates for the unidirectional fluxes. The difference in the network model's representation of these unidirectional fluxes results in fluxes between the extracellular space and the remaining cell compartment which are half the value of those in Huf and Howell's simulation. The following explains why this should be expected. For this illustration, a pump operates as pictured in Fig. 1 *B*, pumping the diffusible material from left to right (forward). In the compartmental system, the forward and backward fluxes are $j_f = k_{LR}S_L = C_L/R_f$, and $j_b = k_{RL}S_R = C_R/R_b$, where $R_f = 1/k_{LR}V_L$ and $R_b = 1/k_{RL}V_R$. In the pump-leak case, as was modeled by the network, the pump produces only a forward flux of magnitude $J_f = C_L/R_p$, and the parallel leak pathway has both a forward and a backward component, but the net flux is $J_L = (C_r - C_L)/R_L$. Both representations must result in the same net flux, so that

$J_{net} = C_L/R_f - C_R/R_b = C_L/R_p - (C_R - C_L)/R_L$. From this comparison, if the value of the leak pathway resistance (R_L) is chosen to be equal to R_b in the other representation, the pump resistance, R_p must be $R_p = R_f R_b/(R_b - R_f)$. The ratio of the forward flux, j_f, to the pump flux, J_f, is $j_f/J_f = R_b/(R_b - R_f)$, and the ratio of the backward flux, j_b, to the leak flux, J_L, is $j_b/J_L = C_R/(C_R - C_L)$. In the case of the strong pump, $j_f/J_f = 20/(20 - 0.2) \cong 1$, whereas for the weak pump, $j_f/J_f = 1/(1 - 0.5) = 2$.

APPENDIX II

Simulation of the Network using SPICE2

Although most of the work reported here was simulated with ASTEC, because SPICE2 is generally more available, the simulation will be described for that program. (The two are very similar, and the program PCAP could easily be substituted with only slight modifications [see footnote 2]). The program for performing the simulations described in this paper using the program SPICE2 is:

```
.TRAN      1S    120    S          UIC
R1    1    2     10     MEG
R2    1    3     10     MEG
R3    2    3     10     MEG
R4    2    5     125    MEG
R5    3    5     20     MEG
R6    3    4     50     MEG
R7    4    5     1      MEG
R8    5    6     0.5    MEG
CG2   2    0     0.1    U          IC = 0
CG3   3    0     0.5    U          IC = 0
CG4   4    0     4      U          IC = 0
CG5   5    0     0.5    U          IC = 0
V1    1    0     PULSE 0.0    0.010    40   1NS   1NS   40   805
V2    7    0     0.115
G1    3    5     3      0     5   U
G2    4    5     4      0     1   U
.PRINT TRAN       V(1)   V(2)   V(3)   V(4)   V(5)   V(6)   I(V1)   I(V2)
.PLOT TRAN        V(1)   V(2)   V(3)   V(4)   V(5)   V(6)   I(V1)   I(V2)
.END
```

The procedure of translating Fig. 5 into the simulation program is straightforward. Each branch is named, for example R1, and then the nodes between which it is connected are listed, e.g. 1 2, positive first (determines the direction of positive current flow through the branch from the positive node to the negative node). The node connections are followed by the value of the element in the case of resistors, and also by an initial value of the potential in the case of capacitors. (Also, in this paper, in order not to confuse the symbols for capacitance and concentrations, gamma has been used for capacitance. The program requires a C as the first letter in a capacitor's name.) Independent voltage sources $V1$ and $V2$ clamp the baths at the 115 mM value and at zero for 40 s, then at 10 mM for 40 s (with a 1 ns rise time), and zero for 40 s (with a 1 ns fall time). For convenience this system was simulated with a simulation time scale measured in seconds but 1 s of simulation represents 1 min in actual time.

The most powerful aspect of the simulation program is in the controlled sources, linear and nonlinear. In SPICE2 these can be used to "generate" currents and/or voltages that depend on currents and/or voltages anywhere in the network as long as the functional dependence can be represented by combinations of multivariable polynomials. In PCAP, other nonlinear functions are possible and both will handle a Michaelis-Menten (saturable) current-voltage characteristic. In this simulation, linear-dependent sources were used for the pumps. For example, the current source

G_1 (a "pump") connected between nodes 3 and 5 (3 positive) depends linearly on the potential between node 3 and ground (0) and its current output is 5×10^{-6} times that voltage. The other cards in the program, each beginning with a dot, are for controlling the simulation. The .TRAN card specifies that a transient analysis is to be carried out. The entries 1S, 120S, and UIC specify the time-step size and duration of the simulation and allow the setting of initial conditions for the capacitors. SPICE2 then solves the network, including the differential equations (four in this case) which never need to be written explicitly.

The simulation procedure might resemble the simulations done on analog computers, at first glance. This is only partially true, because using of the controlled sources and models of solid-state devices, we could produce elements having many characteristics either difficult or impossible to generate with hardware. Within the accuracy of the program, the elements are all ideal so that the simulation cannot be distorted by an imperfect piece of hardware. This mode of simulation is cheap and quick and is replacing "breadboarding" in the electronics industry. For this reason, one can anticipate that the programs will soon be updated and increased in power. (One illustration in the PCAP user's manual is the simulation of an analog computer solving Van der Pol's equation complete with phase plane analysis!)

REFERENCES

BAROCAS, M. 1977. ASTEC2 User's Manual (in French). Compagnie Internationale de Services Informatique, Gif/Yvette, France.

BLATTNER, D. J. 1976. Choosing the right programs for computer-aided design. *Electronics.* April 29. 102–105.

COBELLI, C., A. POLO, and G. ROMANIN-JACUR. 1977. A computer program for the analysis of controllability, observability, and structure identifiability of biological compartmental systems. *Comput. Programs Biomed.* **7**:21–36.

CHUA, L., P. LIN. 1975. Computer Aided Analysis of Electrical Circuits: Algorithms and Computational Techniques. Prentice-Hall, Inc., Englewood Cliffs, N.J.

FARQUHAR, M. G., and G. E. PALADE. 1965. Cell junctions in amphibian skin. *J. Cell Biol.* **26**:263–291.

FINKELSTEIN, A., and A. MAURO. 1963. Equivalent circuits as related to ionic systems. *Biophys. J.* **3**:215–237.

GARY-BOBO, C. M., D. C. MIKULECKY, S. R. THOMAS, H. GOUDEAU, and J. WIETZERBIN. 1978. A network thermodynamic model for short circuit current transients in frog skin during low concentration pulses of NaCl against a zero Na^+ background. *Fed. Proc.* **37**:515.

HEINRICH, R., S. M. RAPOPORT, and T. A. RAPOPORT. 1977. Metabolic regulation and mathematical models. *Prog. Biophys. Mol. Biol.* **32**:1–82.

HELMAN, S. I., and R. S. FISHER. 1977. Microelectrode studies of the active Na transport pathway of frog skin. *J. Gen. Physiol.* **69**:571–604.

HOWELL, J. R., and E. G. HUF. 1974. Model studies on Na* wash-out kinetics in frog skin epidermis. *Comput. Biomed. Res.* **7**:590–599.

HOWELL, J. R., and E. G. HUF. 1975. Metabolic compartmentation in amphibian skin epidermis: A computer simulation study. *Comput. Biomed. Res.* **8**:72–87.

HOWELL, J. R., and E. G. HUF. 1976. Mathematics of non-steady state uptake and release of Na* in a frog skin epidermis model. *Comput. Biol. Med.* **6**:121–131.

HOWELL, J. R., and E. G. HUF. 1977. Numerical simulation of Na* wash-out rates in whole frog skin. *Ann. Biomed. Eng.* **5**:194–207.

HUF, E. G., and J. R. HOWELL. 1974*a*. Computer simulation of the response of frog skin epidermis to changes in $[Na^+]_0$. *J. Membr. Biol.* **15**:67–86.

HUF, E. G., and J. R. HOWELL. 1974*b*. Computer stimulation of Na* wash-out kinetics in frog skin epidermis. *J. Membr. Biol.* **15**:87–106.

HUF, E. G., and J. R. Howell. 1976. Computer analysis of the Na^+ shunt pathways in frog skin epidermis. *Comput. Biomed. Res.* **9**:11–20.

HUF, E. G., and J. R. HOWELL. 1977. Computer modelling: Application to studies on the initial rate of Na^+ uptake by frog skin epidermis. *J. Theor. Biol.* **65**:653–669.

HUF, E. G., D. C. MIKULECKY, and S. R. THOMAS. 1978. A network thermodynamic approach to compartmental analysis. *Fed. Proc.* **37**:705.

KAPLAN, G. 1975. Computer aided design. *I.E.E.E. Spectrum.* October. 40–47.

MIKULECKY, D. C. 1977. A simple network thermodynamic method for series-parallel coupled flows. II. The

non-linear theory, with applications to coupled solute and volume flow in a series membrane. *J. Theor. Biol.* **69:** 511–540.

MIKULECKY, D. C. 1978. A network thermodynamic 2-port for coupled salt and current flow: an improvement over equivalent circuit models. *Fed. Proc.* **37:**705.

MIKULECKY, D. C. and S. R. THOMAS. 1977. A Simple Network Thermodynamic Method for Modelling Linear and Non-Linear Systems of Series-Parallel Coupled Flows Through Physiological Tissues. Proceedings of the 20th Midwest Symposium on Circuits and Systems. K. S. Chao and R. Saeks, editors. Western Periodical Company, North Hollywood, Calif. 139–155.

MIKULECKY, D. C. and S. R. THOMAS. 1978. A simple network thermodynamic method for series-parallel coupled flows. III. Application to coupled solute and volume flows through epithelial membranes. *J. Theor. Biol.* **73:** 697–710.

MIKULECKY, D. C., S. R. THOMAS, C. M. GARY-BOBO, H. GOUDEAU, and J. WIETZERBIN. 1977*a*. Network models of epithelia: Transient changes in short-circuit current resulting from pulses of sodium chloride on the mucosal side and solute and volume transport across kidney proximal tubule. North Atlantic Treaty Organization Research Grant #1239, Report.

MIKULECKY, D. C., W. A. WIEGAND, and J. S. SHINER. 1977*b*. A simple network thermodynamic method for modelling series-parallel coupled flows. I. The linear case. *J. Theor. Biol.* **69:**471–510.

MOREL, F., and G. LEBLANC. 1975. Transient current changes and Na compartmentalization in frog skin epithelium. *Pflugers Arch.* **358:**135–157.

OSTER, G., and A. PERELSON. 1974*a*. Chemical reaction dynamics. I. Geometrical structure. *Arch. Ration. Mech. Anal.* **55:**230–274.

OSTER, G., and A. PERELSON. 1974*b*. Chemical reaction dynamics. II. Reaction networks. *Arch. Ration. Mech. Anal.* **57:**31–98.

RICK, R. A. DÖRGE, E. VONARNIM, and K. THURAC. 1978. Electron microprobe analysis of frog skin epithelium: Evidence for a syncytial sodium transport compartment. *J. Membr. Biol.* **39:**313–331.

SANDBERG, I. W. 1977. On the mathematical foundations of compartmental analysis in biology, medicine, and ecology. Proceedings of the 20th Midwest Symposium on Circuits and Systems. K. S. Chao and R. Saeks, editors. Western Periodical Company, North Hollywood, Calif. 532–537.

THOMAS, S. R. 1977. Network thermodynamic modelling of transepithelial salt and water flow. Ph.D. Thesis, Medical College at Virginia, Richmond, Va.

THOMAS, S. R., and D. C. MIKULECKY. 1978*a*. Transcapillary solute exchange. A comparison of the Kedem-Katchalsky convection-diffusion equations with the rigorous non-linear equation for this special case. *Microvasc. Res.* **15:**207–220.

THOMAS, S. R., and D. C. MIKULECKY. 1978*b*. Network thermodynamic modelling of transepithelial salt and water flow. The kidney proximal tubule. *Am. J. Physiol.* In press.

THOMAS, S. R., and D. C. MIKULECKY. 1978*c*. A network thermodynamic analysis of transepithelial salt and water flow. A model of mammalian proximal tubule. *Fed. Proc.* **37:**287.

WELCH, G. R. 1977. On the role of organized multienzyme systems in cellular metabolism: A general synthesis. *Prog. Biophys. Mol. Biol.* **32:**103–191.

WYATT, J. L., JR. 1978. Network representation of reaction-diffusion systems far from equilibrium. *Comput. Programs Biomed.* In press.